9A.4 CHARACTERISTICS OF CANOPY TURBULENCE DURING THE TRANSITION FROM CONVECTIVE TO STABLE STRATIFICATION

Eva van Gorsel *, J.J. Finnigan, I.N. Harman and R. Leuning
CSIRO, Marine and Atmospheric Research, Canberra, ACT, Australia

1. INTRODUCTION

Increasing atmospheric stability is known to suppress turbulent mixing and often leads to a decoupling of above and in-canopy flows. Understanding of the dynamics that lead to a decoupling and knowledge of the characteristics of in-canopy flows is of particular importance when interpreting nocturnal exchanges of CO2 and trace fluxes.

L.F. Richardson (1920) was the first to state that turbulence in the atmosphere should die away if the static stability exceeds the square of the mean shear. G.I. Taylor (1931) then was able to demonstrate that for certain idealized flows this would happen when local Richardson numbers exceed ¼. Later Miles (1961, 1986) and Howard (1961) generalized Taylor's results to a large class of inviscid stably stratified fluids in steady shear flows.

Raupach et al. (1996) argued that the active turbulence near the top of a forest canopy is patterned on a plane mixing layer, which forms around the inflected mean velocity profile. The strong shear at canopy top allows for hydrodynamic instabilities to form. In the canopy, however, the different transport mechanisms of heat and momentum at leaf level, lead to wind speed profiles that approach the leaf surface value of zero much faster than air temperature approaches the leaf surface temperature (Belcher et al. 2008). When the atmosphere above the canopy is stably stratified, this difference in wind and temperature gradients results in supercritical Richardson numbers below the canopy top and a collapse of in-canopy turbulence.

We discuss observed flow characteristics; show how they change in the transition from the convective to the stable boundary layer and how they can be explained by existing theory. We further discuss implications for ecosystem scale measurements.

2. SITE AND OBSERVATIONS

Tumbarumba flux station is located in the southeastern highlands of New South Wales, Australia (Leuning et al., 2005). The site is in relatively complex terrain (Fig. 1), leading to a variation of −6° to +2° in the angle between the mean wind vector and the azimuthal-average vertical direction (Finnigan et al., 2003). Dominant species in the 40 m tall, open wet sclerophyll forest are *Eucalyptus delegatensis* R.T.Baker and *Eucalyptus dalrympleana* Maiden. The leaf area index (Lai) of the trees is 1.4 $m^2\ m^{-2}$, while the understorey is sparsely covered with shrubs and grass which have a Lai of 1.5 $m^2\ m^{-2}$ (Keith, personal communication). The site

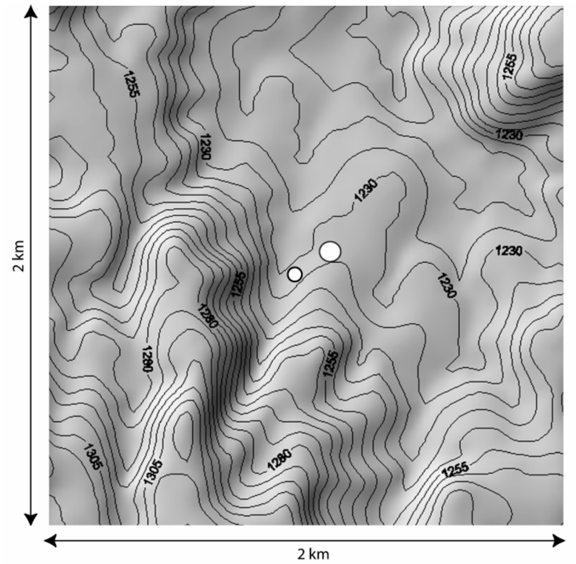

Figure 1. 2 x 2 km^2 topographic map of the Tumbarumba field site showing the location of the main tower (big circle) and the smaller in-canopy tower (small circle). The contour interval is 5 m.

is relatively homogeneous in terms of species composition, density and tree height within a radius of more than 5 km.

At the 70m high main tower we continuously measure profiles of temperature and wind components in 9 heights [0.5, 4.5, 10.5, 18.5, 26.5, 34.5, 42.5, 54.5, 70 m]. The measurements are carried out with Type T thermocouples and 2D Windsonics and 1Hz data is stored. At the tower top an ultra sonic anemometer thermometer (Type HS, Gill Instruments Ltd., Lymington, UK) measures all wind components and virtual temperature at 20 Hz. For a special intensive measurement campaign in November 2006 a second 11m high tower was situated on a nearby slope and in-canopy turbulence was measured simultaneously with 3D Sonics at 7 heights [0.8, 1.4, 2.2, 2.9, 4.4, 5.8, 10.8 m] (Sonics were Type HS, Gill Instruments Ltd., Lymington, UK and CSAT3, Campbell Scientific, Logan, USA, alternating with a CSAT3 in 10.8 m). All raw 20Hz data was stored.

* *Corresponding author address:* Eva van Gorsel, CSIRO Marine and Atmospheric Research, Pye Laboratory, GPO Box 3023, Canberra ACT 2601; Australia. e-mail: eva.vangorsel@csiro.ch

3. METHODS

To calculate the Fourier spectra we applied linear detrending and a Hamming window to the time series. For graphical purposes Fourier transformed time series were averaged into 120 logarithmic bands. Maxima however were calculated on the basis of raw spectra.
Richardson numbers (*Ri*) were calculated as bulk Richardson numbers, approximating local gradients by using finite differences across layers. To test the sensitivity of using linear interpolation or cubic splines to calculate *Ri* we used data from 7.11 – 12.11.2006. Calculated *Ri* at canopy top differed by 13% on average. To assess the instrumental uncertainty we used data from the same time period where both 2D and 3D Sonics were measuring at the main tower. We used either profiles to calculate *Ri* and could attribute another 10% uncertainty to the instruments.
To calculate phase averages of temperature and associated vertical wind velocity fluctuation (Fig. 8) we applied linear detrending on 1 h runs and low pass filtered the temperature time series (small tower, 11 m) with moving averages of 45 s (Finnigan et al. 1984). We searched for zero crossings and discarded occurrences where dT/dt > 0. We then averaged the original unsmoothed time series of all variables of interest around the detected, valid zero crossing points over a window size of ± 60 s.

4. RESULTS

During daytime, turbulence leads to strong temperature variations in the canopy (Figures 2 and 3). The magnitude of these fluctuations generally decreases in the late afternoon. We might expect that turbulence levels would stay low throughout the night as in this relatively open canopy stable nighttime stratification leads to a suppression of the total

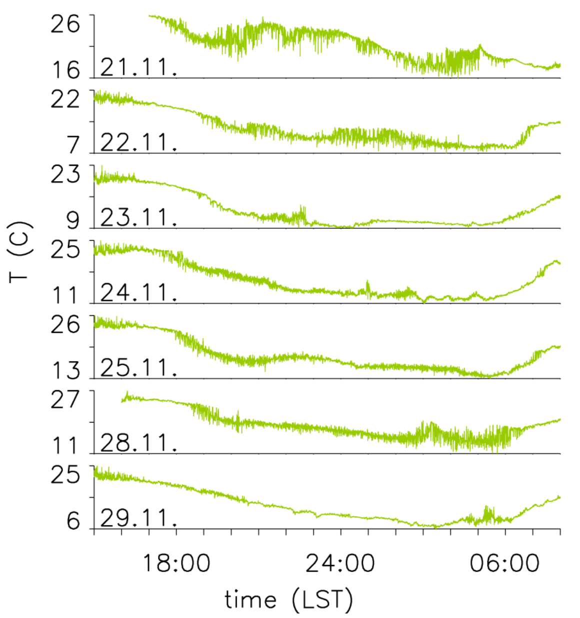

Figure 2. 1Hz time series of temperature measured at 10.8 m height at the small tower. At 26.11 and 27.11. the measurement system was powered down.

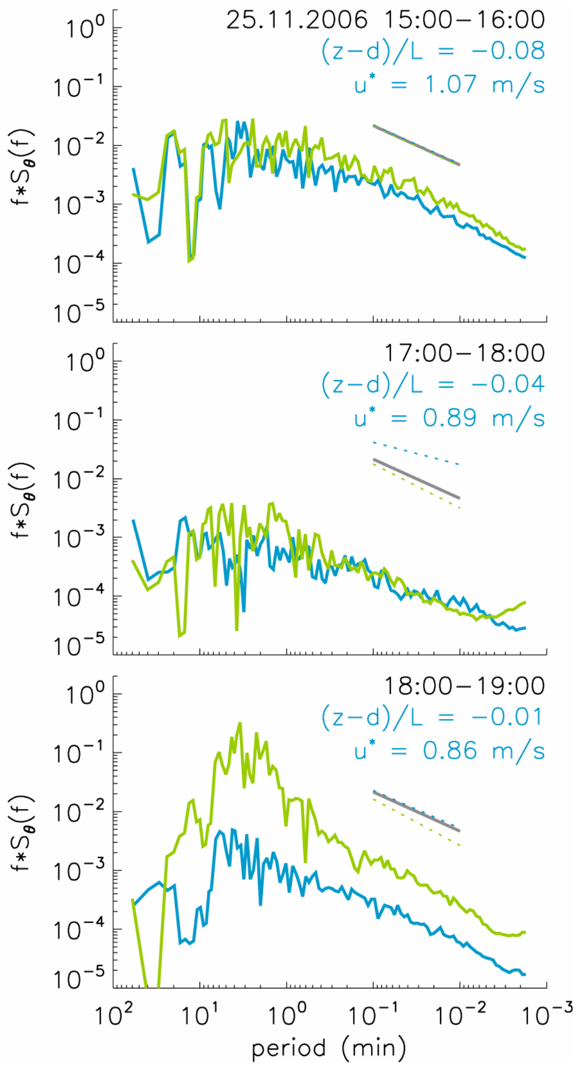

Figure 3: Fourier spectra of in (green/light grey) and above canopy (blue/dark grey) temperatures. The solid line stands for -2/3 slope the dotted lines are fitted to the respective spectra.

turbulent kinetic energy. Observations however show that on all but one night there are either periods when large amplitude temperature fluctuations are observed (e.g. 23.11), or where such fluctuations are observed throughout the night (21., 22., 25. and 28.11.).
As an example we will investigate the transition from the convective to the stable boundary layer on the 25.11.2006 and also analyze the night of the 28.11.2006. During this night a transition occurs from moderate above-canopy stability to neutral conditions.
Figure 3 and Table 1 summarize some of the flow characteristics of the 25.11.2006. Above-canopy flow is slightly unstable in the afternoon and strong dynamic turbulence leads to increasingly neutral conditions towards the evening. High friction velocities (*u**) are observed throughout this time period. The 15:00-16:00 temperature spectra have inertial subrange slopes close to -2/3. In the 17:00-18:00 spectra the total variance is quite small and white noise is observed at the high frequency end of the in canopy spectrum. The main energy in this spectrum is from periods > 1 minute. This is exaggerated in the

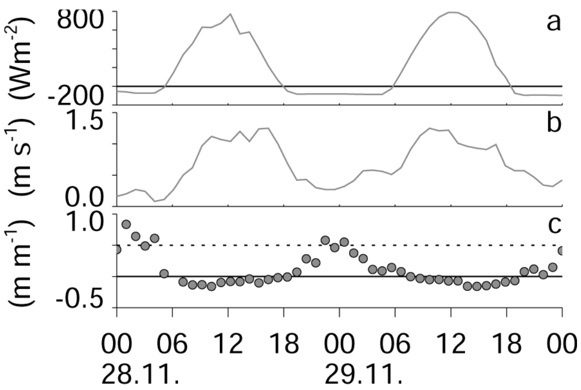

Figure 4. time series of a) net radiation b) the fricition velocity u^* and c) the dimensionless Monin-Obhukov length *(z-d)/L*. All measurements were taken at the main tower in 70 m height.

18:00-19:00 run, where 14% of the total energy is located in the periods between 3.08 and 3.75 min. (with the maximum variance at 3.43 min). Due to large in canopy temperature gradients the total amount of variance is much higher in than above the canopy. In the canopy spectral slopes with a faster roll of that -2/3 are observed. Turbulent fluctuations here do work against drag and lose kinetic energy to heat and wake kinetic energy therewith shortcutting the spectral cascade (Finnigan, 2000).

Table 1: shows the total temperature variance and the slopes measured in the inertial subrange of the above and sub canopy temperature spectra. The ratio of the maximum variance measured in a single frequency band to the total variance can be interpreted as a measure for monochromaticity.

	time	above canopy	sub canopy
variance(θ) (°C²)	15:00-16:00	0.12	0.15
	17:00-18:00	0.02	0.05
	18:00-19:00	0.01	0.42
slope ( )	15:00-16:00	-0.66	-0.68
	17:00-18:00	-0.38	-0.75
	18:00-19:00	-0.66	-0.79
$S_{(max)\theta}/\sigma^2(\theta)$ ( )	15:00-16:00	0.03	0.02
	17:00-18:00	0.01	0.05
	18:00-19:00	0.03	0.14

Above canopy turbulence statistics do not indicate the very different flow characteristics that prevail above and in the canopy. This is also confirmed for the 28.11.-29.11.2006.

No clear sky conditions were observed on the 28.11. (Fig. 4). Dynamic turbulence was fairly strong throughout the night and increased after midnight, shifting the flow from weakly stable to neutral conditions. Figure 5 gives a more detailed picture of the stability classes through the whole canopy. Above-canopy Richardson numbers (*Ri*) confirm that the flow was weakly stable but subcritical during most of the night, except during a short period when weakly stable but supercritical *Ri*'s were observed. In the

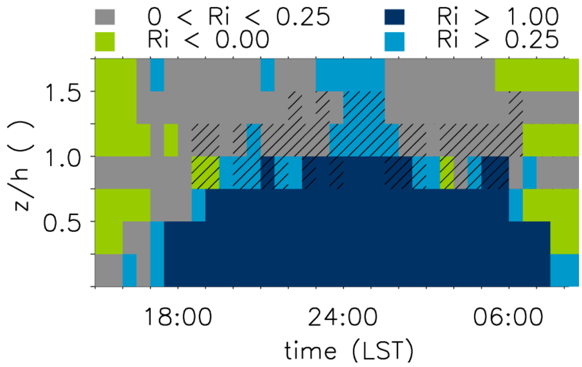

Figure 5. time series of Richardson gradient numbers through the canopy as measured on 28./29.11.2006. The height (y-axis) is normalized with canopy height (*h*). The Richardson numbers (*Ri*) have been classified into unstable (*Ri*<0), weakly stable subcritical (0<*Ri*<0.25), weakly stable supercritical (1>*Ri*>0.25) and strongly stable (*Ri*>1). The hatched area indicates the estimated height of the critical level.

canopy the situation differs quite dramatically but in agreement with arguments by Belcher et al. (2008) who attribute high *Ri* to different transport processes of heat (molecular transport) and momentum (pressure transport) at leaf scale. This leads to a faster decrease of wind speed than of temperature into the canopy and hence to stable flow conditions. The observations show that conditions at canopy top are indeed supercritical with few exceptions in the early morning when strong shear leads to enhanced mixing. Deeper in the canopy very stable conditions were observed throughout the night.

At canopy height wind shear is often sufficiently strong to cause *Ri* to drop below its critical value. This situation allows Kelvin–Helmholtz waves to form (Raupach et al. 1996). These waves in turn can propagate in the adjacent air above and below. A critical level, where 0<*Ri*<¼, exists for gravity waves that are excited by wind shear (Howard, 1961) and at this height the horizontal phase speed of the wave

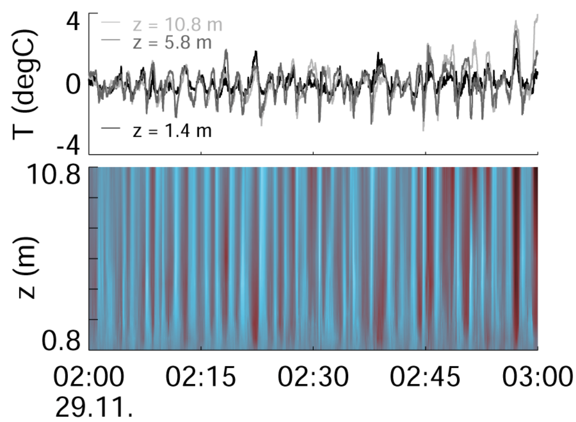

Figure 6. top panel: time series of temperature fluctuations on 29.11.2006 02:00-03.00 for 3 selected heights. The bottom panel shows contours of the temperatures from all seven measurement heights ranging from -2.68 °C (light blue or grey) to 3.94 °C (dark red or grey). The mean has been subtracted from each time series.

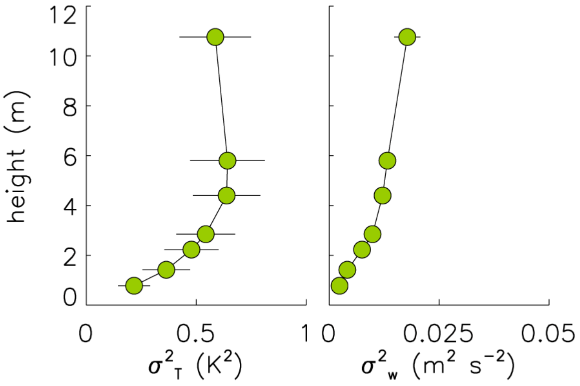

Figure 7. Average profiles of σ^2_T (left panel) and σ^2_w (right panel) in the sub-canopy for the time period 28.11.2006 20:00 - 29.11.2006 05:00.

matches the flow speed. We can further expect alignment between the mean wind and the direction of wave propagation (Lee and Barr, 1998). To test for such a critical level we used the temperature time series from 10 m at both towers and calculated the measured lags in peak correlation between them. We

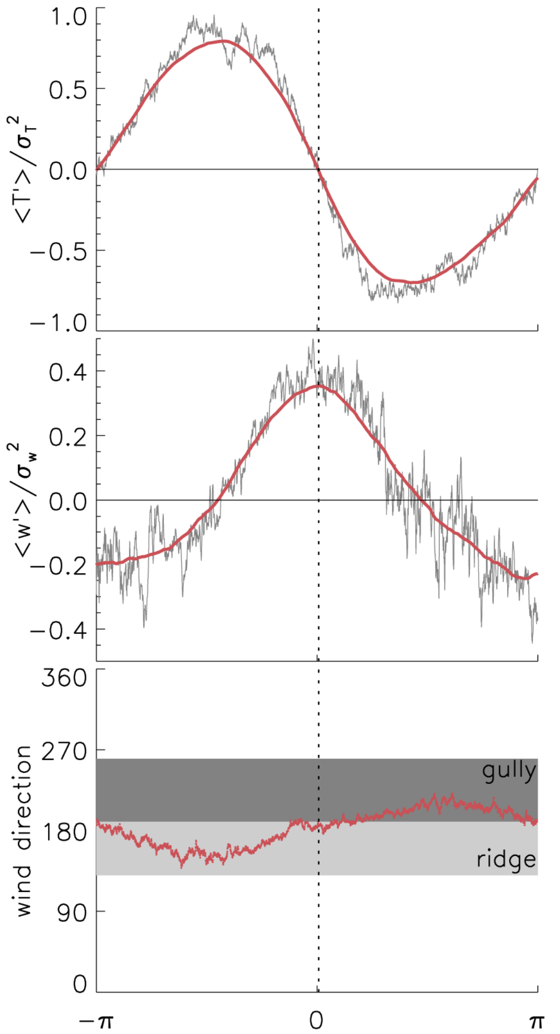

Figure 8. normalized conditional averages of temperature *T*, vertical velocity (*w*) and wind direction. Red thick lines in the first two panels are smoothed with 30 s running means. Total window with is 120 s. Same time period as Figure 7.

then used wind velocity and direction measured at the large tower to calculate the expected lag for each level. The critical level is located where the calculated and expected lags agree with each other. This layer is indicated by the hatched area in Figure 5. Confirming theoretical expectation with experimental evidence all calculated height intervals with the critical level include or are adjacent to the canopy top, where due to the inflection in the wind profile shear is largest.

Figure 6 confirms that the time series have little low frequency content. Large parts of the air column undergo vertical oscillations simultaneously resulting in highly coherent temperature fluctuations that are dampened only in the very proximity of the ground. The period of temperature oscillations (p) through the canopy is $p = 122 \pm 9$ s. The small standard error confirms the coherency of the oscillations. Carruthers and Hunt (1986) have have applied rapid distortion theory to calculate the structure of turbulence in an unsheared, stably stratified layer below adjoining a sheared turbulent region. This matches approximately the situation in the canopy at night. The theory showed that eddies with frequencies of the same order as the buoyancy frequency N of the stratified layer were least affected by the stratification and waves with higher frequencies decayed rapidly with distance from the interface. The measured buoyancy period (defined as $P_{BV} = 2\pi/N$) increased from 93 ± 23 s (02:00-02:30) to 102 ± 23 s (02:30-03:00) in the stably stratified layer reflecting the decreasing stability. To the authors knowledge theory has not been extended to situations where $N(z) \neq$ const but the observations indicate that the sub-canopy periodicity is equal to P_{BV} within the standard errors.

The amplitudes of temperature oscillations have a maximum at 5 m height as shown by the vertical profile of temperature variances (Fig. 7). This results from the non-constant temperature gradient in the canopy and decreasing displacement distance of air parcels due the presence of the ground as indicated by decreasing σ^2_w with decreasing height.

Linear gravity waves generally have a phase shift of ± 90° between the vertical wind component and scalars. But wave-turbulence interaction can lead to different phase shifts and hence to scalar fluxes (Fitzjarrald and Moore, 1990, Lee et al., 1997, Cava et al., 2004) and net energy exchange (Finningan, 1988, Finnigan et al., 1984, Einaudi and Finnigan, 1993). Figure 8 shows the normalized conditional averages of temperature *T*, vertical velocity *w* and wind direction for the time period 28.11.2006 20:00 - 29.11.2006 05:00. On average temperature and vertical wind have a phase shift close to 90°. Air parcels that are displaced upwards are increasingly cooler and warming is associated with downward movement. There is an accompanying oscillation in wind direction. Air coming from a nearby ridge (Fig. 2) is warmer on average, whereas colder air masses come from a nearby gully.

Spectra confirm that for periods that are less stable, within-canopy temperature fluctuations are larger than those observed above the canopy (Fig. 9). This is not the case for vertical velocity fluctuations, as

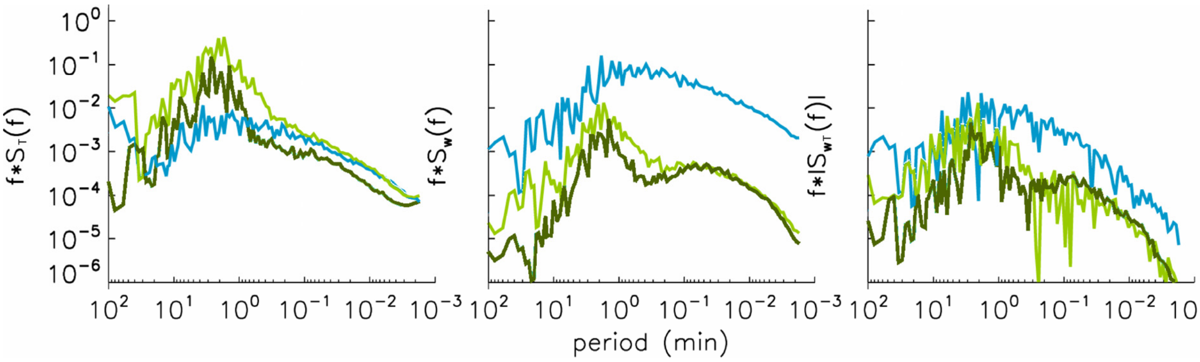

Figure 9. spectra of temperature θ (left panel), vertical wind w (middle panel) and cospectrum $w\theta$ (right panel). In canopy spectra (11 m) are depicted for the time periods from 23:00-01:00 and 03:00-05:00 (dark green and light green or grey respectively) above canopy spectra (70 m) are shown for the time period 03:00-05:00 only (blue/ medium grey).

momentum is absorbed as aerodynamic drag on the foliage leading overall to less vertical kinetic energy with decreasing height into the canopy. The within-canopy cospectra $\overline{w'T'}$ are smaller than their above canopy counterpart. Again this is particularly pronounced at the higher frequencies. Lower frequency covariance between the two variables shows that the phase shift is not exactly 90° and that the waves are not linear waves. The wave induced flux $\langle w'\rangle\langle T'\rangle$ contributes 17% to the total heat flux $\overline{w'T'}$.

In both spectra and cospectra we observe an increase in low frequency energy between the first (23:00-01:00) and the second (03:00-05:00) time interval. As shown in Figure 4 above canopy flow shifts from slightly stable to neutral during this time. The existence of a neutrally stratified layer above the strongly stratified canopy insures a layer centred around a critical level with 0<*Ri*<¼ and wave growth. Chimonas (1972) has shown also that if turbulence is present, momentum and energy from the background can flow into the wave, causing the wave amplitude to increase (Chimonas (1972)). This is accompanied by a broadening of the spectrum as a wider range of wavelengths is supported by stability conditions.

5. DISCUSSION AND IMPLICATIONS FOR ECOSYSTEM SCALE FLUX MEASUREMENTS

During some time periods we have observed supercritical Richardson numbers at all levels and still found that while turbulence was suppressed, oscillations with periods of about 2 min could be observed. A simple explanation for this is the spatial resolution of the measurements. It is possible that sub-critical *Ri* was reached but not measured. It is also possible that the presence of the canopy further destabilises the flow. There are studies showing that the presence of the ground has a destabilizing effect on Kelvin-Helmholtz waves in the atmosphere (Lalas et al. 1976). But linear theory has not been extended to investigate the role of drag or non constant $N(z)$ on stability.

The occurrence of waves in the canopy challenges nighttime measurements of ecosystem scale flux measurements of e.g. CO2. The source sink term of a scalar <*S*> can be estimated by

$$\langle S\rangle = \underbrace{\overline{c_d}\,\overline{w'\chi_s'}}_{\mathrm{I}} + \underbrace{\int_0^{h_c}\overline{c_d}\,\frac{\partial\overline{\chi_s}}{\partial t}\,dz}_{\mathrm{II}} + \underbrace{\frac{1}{L^2}\int_0^{L}\int_0^{L}\int_0^{h_c}\left[\overline{uc_d}\,\frac{\partial\overline{\chi_s}}{\partial x} + \overline{vc_d}\,\frac{\partial\overline{\chi_s}}{\partial y} + \overline{wc_d}\,\frac{\partial\overline{\chi_s}}{\partial z}\right]dzdydx}_{\mathrm{III}} \qquad (1)$$

where x, y, z define the Cartesian coordinates χ_s is the mixing ratio of the molar density of the scalar (c_c) to dry air (c_d) (Leuning, 2004). The first term on the RHS of eq 1 is the eddy flux of the scalar. We have shown that the wave induced heat flux in the canopy contributes 17% to the total flux. To minimize the error introduced by not capturing complete wave cycles long averaging times are required.

The second term on the RHS of eq 1 is the change in storage term. It is ideally calculated as the difference of the spatially averaged instantaneous profile at the beginning and end of the averaging period of <*S*> (Finnigan, 2006). In practise we commonly measure one profile only and average over say 5 min around the end of the hour to reduce random error. If (by adjusting the flow rates) the profile is measured simultaneously at all heights, knowledge of oscillation periods could help to minimize random errors by choosing suitable averaging times. If different levels of the profiles are measured subsequently, scalar fluctuations will result in 'kinky' profiles and bigger random errors.

Measuring horizontal gradients probably poses the biggest challenge. An ideal measuring cycle will depend on wave direction and propagation speed and therefore be quite variable. Measured gradients will be due to different air masses as well as phase differences.

Vertical advection is usually derived from average concentrations measured at reference height (typically twice the canopy height) and averages of the concentrations of the total air column below reference height. As for the turbulent flux, averaging intervals need to be long to minimize errors introduced by not ending on a complete wave cycle.

We have shown that when the flow shifts from slightly stable to neutral above the canopy, a critical level and strong wave growth occurs. This may be augmented because the presence of turbulence can aid the flow of momentum and energy from the background into the wave. This is important as it is common practise to filter ecosystem data using above-canopy u^* as a substitute for turbulent mixing. When turbulent mixing is strong it is assumed that term III of eq 1 is small compared to the sum of terms I and II and that this data can be used for constraining models. Data with high u^* values and close to neutral above canopy conditions however would have the largest random errors if in canopy stability is maintained.

6. CONCLUSIONS

In the canopy the stratification can be very stable with supercritical Richardson numbers (*Ri*) while above canopy flow is neutral to slightly stable. High in canopy stability can be explained by different transport processes of heat and momentum at leaf level scale. They lead to a faster decrease of wind speed than of temperature into the canopy (Belcher et al. 2008). A collapse of in-canopy turbulence follows as all oscillations with frequencies higher than the Brunt Väisälä *N* in the stable layer decay rapidly with distance from the interface where the instability is initiated. We have shown that this critical level is located close to canopy top, the height where shear is largest.

Clearly the effect of canopy waves should be taken into account when designing experiments and analysing data to determine ecosystem fluxes at canopy scale.

ACKNOWLEDGEMENTS

The authors would like to acknowledge Dale Hughes, Mark Kitchen and Steve Zegelin for ongoing support in maintenance and expansion of the flux station as well as for data transfer, processing, control and archiving. We are grateful to the Forestry Department, New South Wales, for permission to install the flux station in the Bago State Forest. This work was supported in part by a grant from the Australian Greenhouse Office (1999–2008) through the Australian Climate Change Science Program and its predecessors.

REFERENCES

Belcher, S.E., Finnigan, J.J. and Harman, I.N. Flows through forest canopies in complex terrain. Ecol. Applications (accepted).

Carruthers, D.J. and Hunt, J.C.R. 1986. Velocity fluctuations near an interface between a turbulent region and a stably stratified layer. J. Fluid. Mech., **165,** 475-501.

Cava D., Giostra U., Siqueira M., Katul G. 2004. Organized motion and radiative perturbations in the nocturnal canopy sublayer above an even-aged pine forest. Boundary-Layer Meteorol., **112**, 129–127

Chimonas, G. 1970. The extension of the Miles-Howard theorem to compressible fluids. J. Fluid. Mech., **42,** 833-836.

Einaudi, F. and Finnigan, J. J. 1993. Wave-Turbulence Dynamics in the Stably Stratified Boundary Layer. J. Atmos. Sci., **50**, 1841–1864.

Finnigan, J. J. 2006. The storage term in eddy flux calculations. Agric. Forest. Meteorol., 136, 108-113.

Finnigan, J. J., Clement, R., Malhi, Y., Leuning, R. and Cleugh, H. A. 2003.A reevaluation of longterm flux measurement techniques. Part I: averaging and coordinate rotation. Q. J. Roy. Meteorol. Soc. **130**, 1–29.

Finnigan, J. J. 2000. Turbulence in plant canopies. Annu. Rev. Fluid Mech., **32**, 519–571

Finnigan, J. J. 1988. Kinetic Energy Transfer between Internal Gravity Waves and Turbulence. J. Atmos. Sci., **45**, 486–505.

Finnigan, J. J., Einaudi, F., and Fua, D. 1984. The Interaction between an Internal Gravity Wave and Turbulence in the Stably-Stratified Nocturnal Boundary Layer. J. Atmos. Sci., **41**, 2409–2436.

Fitzjarrald, D. R. and Moore, K. E. 1990. Mechanisms of Nocturnal Exchange between the Rain Forest and the Atmosphere. J. Geophys. Res. **95D**, 16839–16850.

Howard, L. N. 1961. Note on a paper by J. W. Miles. J. Fluid Mech., **10**, 509-512.

Lalas, D.P., Einaudi, F. and Fua, D. 1976. The destabilising effect of the ground on Kelvin-Helmholtz Waves in the atmosphere. J. Atm. Sciences., **33**, 59-69.

Lee, X and Barr, A.G. 1998. Climatology of gravity waves in a forest. Q.J.R.Meteorol.Soc., **124**, 1403-1419.

Lee, X. 1997. Gravity Waves in a Forest: A Linear Analysis, J. Atmos. Sci., **54**, 2574–2585.

Leuning, R., Cleugh, H. A., Zegelin, S. J. and Hughes, D. 2005. Carbon and water fluxes over a temperate Eucalyptus forest and a tropical wet/dry savanna in Australia: measurements and comparison with MODIS remote sensing estimates. Agric.For. Meteorol., **129**, 151–173.

Leuning, R. 2004. Measurements of trace gas fluxes in the atmosphere using eddy covariance: WPL corrections revisited. In: Handbook of Micrometeorology. Atmospheric and Oceanographic Sciences Library, Kluwer Academic, Dordrecht/Boston/London, 119–132 pp.

Miles, J. W. 1961. On the stability of heterogeneous shear flows. J. Fluid Mech., **10**, 496-508.

Miles, J. W. 1986. Richardson's criterion for the stability of stratified flows. Physics of Fluids, **29**, 3470-3471.

Raupach, M.R., Finnigan, J.J. and Brunet, Y. 1996. Coherent eddies and turbulence in vegetation canopies: the mixing – layer analogy. Boundary Layer Meteorol., **78**, 351-382.

Richardson, L.F. 1920. The supply of energy from and to atmospheric eddies. Proc. Roy. Soc. London Ser. A, **97**, 354-373.

Taylor, G.I. 1931. Effect of variation in density on the stability of superposed streams of fluid. Proc. Roy. Soc. London Ser. A., **132**, 499-523.